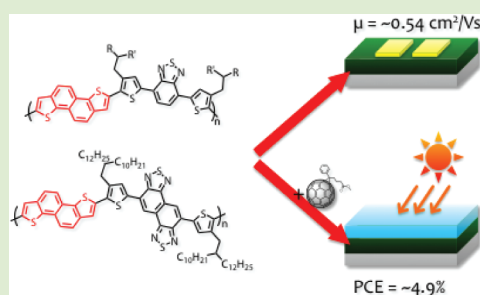


## Naphthodithiophene-Based Donor–Acceptor Polymers: Versatile Semiconductors for OFETs and OPVs

Itaru Osaka,<sup>\*,†,‡</sup> Toru Abe,<sup>†</sup> Masafumi Shimawaki,<sup>†</sup> Tomoyuki Koganezawa,<sup>§</sup> and Kazuo Takimiya<sup>\*,†,||</sup><sup>†</sup>Department of Applied Chemistry, Graduate School of Engineering, Hiroshima University, 1-4-1 Kagamiyama, Higashi-Hiroshima, Hiroshima, 739-8527, Japan<sup>‡</sup>Precursory Research for Embryonic Science and Technology, Japan Science and Technology Agency, Chiyoda-ku, 102-0075, Japan<sup>§</sup>Japan Synchrotron Radiation Research Institute, 1-1-1, Kouto, Sayo-cho, Sayo-gun, Hyogo 679-5198, Japan<sup>||</sup>Institute for Advanced Materials Research, Hiroshima University, Higashi-Hiroshima, 739-8530, Japan

## Supporting Information

**ABSTRACT:** We report the synthesis, characterization, and OFET and OPV properties of a series of novel naphthodithiophene (NDT3)-based donor–acceptor semiconducting polymers. A striking feature of the present polymers is the very close  $\pi$ – $\pi$  stacking of 3.5 Å, most likely as a result of the large  $\pi$  system and the D–A system in the polymer backbone. PNNDT3NTz-DT, in particular, is found to be one of the few examples of versatile polymers that exhibit both the field-effect mobility of  $\sim 0.5$  cm<sup>2</sup>/(V s) and the PCE of  $\sim 5\%$ . These results indicate that NDT3 is a promising versatile core unit for semiconducting polymers and that the use of highly  $\pi$ -extended heteroarenes as both the donor and the acceptor unit is a promising design strategy to develop high performance polymers.



Semiconducting polymers have been attracting considerable attention in organic electronics owing to their solution processability and mechanical properties and, thus, offer a promising pathway to large area and flexible devices, consisting of organic field-effect transistors (OFETs) or organic photovoltaics (OPVs).<sup>1</sup> Recent advances in the development of new semiconducting polymers have achieved field-effect mobilities of  $>1$  cm<sup>2</sup>/(V s)<sup>2</sup> and power conversion efficiencies (PCEs) of  $>7\%$  in bulk heterojunction (BHJ) devices together with fullerene derivatives.<sup>3</sup> An important design strategy to develop high performance polymers is the construction of strong  $\pi$ – $\pi$  stacking between cofacial backbones, which would facilitate the charge carrier transport. The use of donor–acceptor (D–A) systems in the semiconducting polymer backbone, where electron-rich (donor; D) and electron-poor (acceptor; A) units are incorporated into the main chain, is a key technology to promote strong intermolecular interactions and thereby  $\pi$ – $\pi$  stacking, as well as to expand the absorption range, and in turn has emerged as promising materials both for OFETs<sup>4</sup> and OPVs.<sup>5</sup> Incorporation of  $\pi$ -extended heteroaromatic rings (heteroarenes) into the polymer main chain is also beneficial to enhance the intermolecular interaction.<sup>6</sup> It is therefore quite reasonable that the use of such  $\pi$ -extended heteroarenes as either the D or A unit for D–A polymers is highly expected to afford high-performance polymers.

As a family of thiophene-fused heteroarenes, naphthodithiophenes (NDTs) have been of great interest as a core unit for organic semiconductors.<sup>7</sup> Recently, we have reported that naphtho[1,2-*b*:5,6-*b'*]dithiophene (NDT3)-based polymers (PNNDT3BTz) exhibited a mobility as high as 0.77 cm<sup>2</sup>/(V s).

The high performance of PNNDT3BTz is rationalized by the formation of the highly ordered  $\pi$ – $\pi$  stacking structure and the fully distributed HOMO coefficients along the backbone, which might facilitate the carrier transport between the main chains.<sup>8</sup> It is thus expected that the incorporation of NDT3 into D–A backbone systems can lead to semiconducting polymers that show high performances both in OFETs and OPVs, that is, “versatile polymers”. Herein, we report the synthesis and characterization of new NDT3-based D–A copolymers and their OFET and OPV performances.

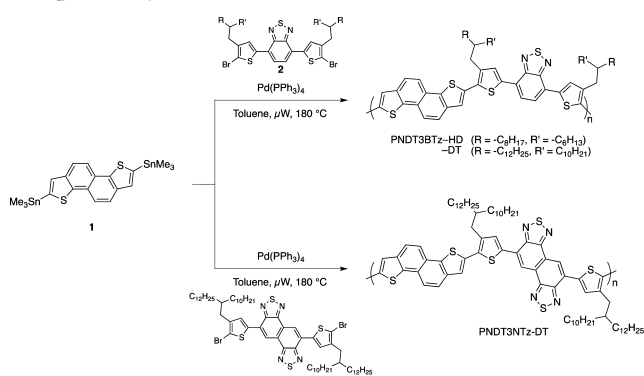
Scheme 1 shows the synthetic routes to the polymers. Benzothiadiazole (BTz), a well-known electron deficient heteroaromatic ring, is introduced as the acceptor unit (PNNDT3BTzs). Naphthobisthiadiazole (NTz),<sup>9</sup> a doubly BTz-fused heteroaromatic ring, is also chosen as the acceptor unit (PNNDT3NTz-DT), with which the polymer includes highly  $\pi$ -extended (four-ring-fused) heteroarenes both as the donor and acceptor and thus is expected to exhibit even higher device performances as compared to the BTz counterpart. Distannylated NDT3 (1) was copolymerized with comonomer 2 or 3, where BTz or NTz is sandwiched by two thiophenes with long branched alkyl chains to yield desired polymers, respectively. It was found that PNNDT3BTz-HD, with hexyldecyl side chains, had limited solubility (soluble in hot chlorinated benzenes) and thus it precipitated during the

Received: February 6, 2012

Accepted: March 5, 2012

Published: March 13, 2012

## Scheme 1. Synthetic Route to the NDT3-Based Donor–Acceptor Polymers



polymerization, resulting in a relatively low molecular weight of  $M_n = 17.0$  kDa (PDI = 1.2). On the other hand, PNNDT3BTz-DT, with longer decyltetradecyl side chains, afforded higher molecular weight of 30.3 kDa (PDI = 1.8), most probably due to the increased solubility, and is soluble in warm (>ca. 40 °C) chloroform and chlorinated benzenes. PNNDT3NTz-DT having decyltetradecyl side chains is found to have  $M_n = 31.0$  kDa with PDI = 10.0 and is soluble in hot (>ca. 100 °C) chlorinated benzenes. The very large PDI for PNNDT3NTz-DT might be attributed to the high tendency to aggregate in the solution, resulting in overestimation of  $M_w$ .<sup>10</sup>

UV–vis absorption spectra of the polymers are shown in Figure 1. In the solution (Figure 1a), PNNDT3BTz-HD exhibits

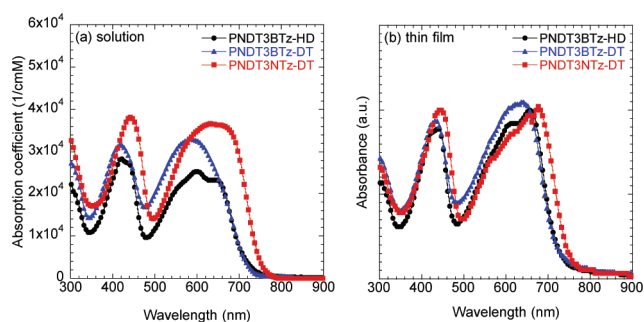


**Figure 1.** UV–vis absorption spectra of the polymers in the solution (a) and in the thin films (b).

an absorption maximum ( $\lambda_{max}$ ) at 600 nm with an additional peak at 650 nm, whereas PNNDT3BTz-DT shows a relatively blue-shifted  $\lambda_{max}$  at 582 nm, implying the stronger aggregation ability of PNNDT3BTz-HD than PNNDT3BTz-DT. Despite the same backbone structure, the absorption coefficient of PNNDT3BTz-DT appears to be larger than PNNDT3BTz-HD, which is possibly related to the difference in molecular weight. PNNDT3NTz-DT, with NTz as the acceptor unit, shows relatively broad absorption and a red-shifted  $\lambda_{max}$  of 632 nm compared to PNNDT3BTzs, most likely due to the much pronounced electron-deficient nature and the more rigid and planar structure of NTz as compared to BTz. The absorption coefficient of PNNDT3NTz-DT is larger than PNNDT3BTzs, as seen in the copolymer of NTz and BTz with the quaterthiophene unit.<sup>9c</sup> In the film (Figure 1b), PNNDT3BTz-DT affords slightly broader spectra and slightly blue-shifted absorption maxima ( $\lambda_{max}$ ) than PNNDT3BTz-HD.  $\lambda_{max}$  of PNNDT3BTz-HD and -DT are located at 658 and 640 nm,

respectively. Nevertheless, the onset wavelength is about 740 nm for both PNNDT3BTzs, which corresponds to the optical bandgap ( $E_g$ ) of 1.7 eV.  $\lambda_{max}$  of PNNDT3NTz-DT was 678 nm with  $E_g = 1.6$  eV, which is red-shifted from that for PNNDT3BTz, as seen in the solution spectra. Ionization potentials (IP) are evaluated by photoelectron spectroscopy in air, and both PNNDT3BTzs give the same value of 5.15 eV, whereas PNNDT3NTz-DT provides 5.25 eV, which can also be explained by the difference in the electron-poor nature.

Top-contact/bottom gate OFET devices were fabricated using polymer thin films spin-coated from *o*-dichlorobenzene solutions onto hexamethyldisilazane (HMDS)- or 1*H*,1*H*,2*H*,2*H*-perfluorodecyltriethoxysilane (FDTS)-treated Si/SiO<sub>2</sub> substrates, which were subsequently annealed at 150 °C. Typical transfer and output curves of the FDTS-treated devices with PNNDT3BTz-DT and PNNDT3NTz-DT are depicted in Figure 2, and mobilities calculated from the

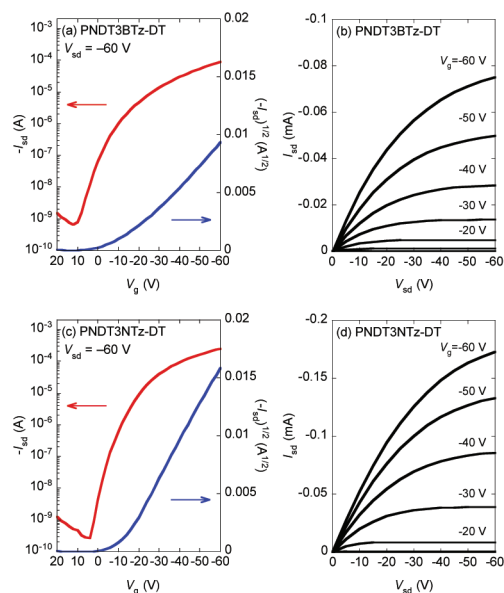


**Figure 2.** OFET characteristics of the polymers: (a,b) transfer and output curves of a PNNDT3BTz-DT-based device; (c,d) transfer and output curves of a PNNDT3NTz-DT-based device. Both devices were fabricated with FDTS-modified Si/SiO<sub>2</sub> substrates.

saturation regime and current on/off ratios are summarized in Table 1. Mobilities for PNNDT3BTz-DT-based devices with the FDTS-treated substrate are as high as 0.12 cm<sup>2</sup>/(V s), whereas those with HMDS-treated devices are slightly lower, ~0.080 cm<sup>2</sup>/(V s). The higher mobility for FDTS-treated devices could be attributed to the better molecular ordering on the substrate surface with lower surface energy compared to HMDS-treated devices.<sup>2b</sup> PNNDT3BTz-HD affords lower mobilities than the longer side chain analogues, ~0.018 cm<sup>2</sup>/(V s) and ~0.050 cm<sup>2</sup>/(V s) with HMDS- and FDTS-treated devices, respectively. The mobilities for PNNDT3NTz-DT are very high, ~0.54 cm<sup>2</sup>/(V s) with the HMDS-treated devices, which is similar to that with the FDTS-treated devices, ~0.41 cm<sup>2</sup>/(V s).

BHJ solar cells were fabricated by spin-coating the polymer/PC<sub>61</sub>BM solutions in *o*-dichlorobenzene (DCB) onto the PEDOT/PSS-coated ITO glasses, followed by vacuum evaporations of LiF and Al as the cathode. Figure 3 depicts the current density–voltage (*J*–*V*) curves and the external quantum efficiency (EQE) spectra of the polymer devices. The

Table 1. OFET and OPV Characteristics of the Polymer-Based Devices

| polymers    | OFETs   |   |                                | OPVs               |   |                     |      |            |  |
|-------------|---|---|--------------------------------|--------------------|---|---------------------|------|------------|--|
|             | $\mu_{\text{HMDS}}$ [ $\text{cm}^2/(\text{V s})$ ] <sup>a</sup> | $\mu_{\text{FDTs}}$ [ $\text{cm}^2/(\text{V s})$ ] <sup>b</sup> | $I_{\text{on}}/I_{\text{off}}$ | $p/n$ <sup>c</sup> | $J_{\text{SC}}$ ( $\text{mA}/\text{cm}^2$ ) | $V_{\text{OC}}$ (V) | FF   | PCE (%)    |  |
| PNDT3BTz-HD | $\sim 0.018$  | $\sim 0.052$  | $\sim 10^6$                    | 1:2                | 7.2   | 0.60                | 0.42 | $\sim 1.8$ |  |
| PNDT3BTz-DT | $\sim 0.080$  | $\sim 0.12$   | $\sim 10^6$                    | 1:1                | 8.4   | 0.70                | 0.64 | $\sim 3.8$ |  |
| PNDT3NTz-DT | $\sim 0.54$   | $\sim 0.41$   | $\sim 10^7$                    | 1:1                | 11.3  | 0.83                | 0.52 | $\sim 4.9$ |  |

<sup>a</sup>Field-effect mobilities in the HMDS-treated devices. <sup>b</sup>Field-effect mobilities in the FDTs-treated devices. <sup>c</sup>Polymer ( $p$ ) to PC<sub>61</sub>BM ( $n$ ) weight ratio.

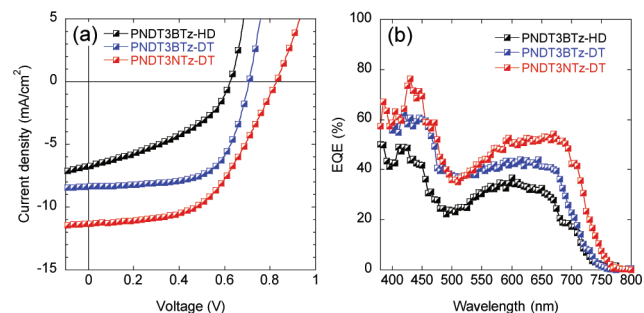


Figure 3. (a)  $J$ - $V$  curves and (b) EQE spectra of the polymer-based BHJ solar cells.

PNDT3BTz-HD device shows low PCEs of  $\sim 1.8\%$  at a polymer to PC<sub>61</sub>BM weight ( $p/n$ ) ratio of 1:2, with short-circuit currents ( $J_{\text{SC}}$ ) of  $\sim 7.2$  mA/cm<sup>2</sup>, open-circuit voltages ( $V_{\text{OC}}$ ) of  $\sim 0.60$  V, and fill factors (FF) of  $\sim 0.42$ . In the meantime, PNDT3BTz-DT, with the longer side chain, exhibits PCEs of  $\sim 3.8\%$  at a  $p/n$  ratio of 1:1, with  $J_{\text{SC}} = \sim 8.4$  mA/cm<sup>2</sup>,  $V_{\text{OC}} = \sim 0.70$  V, and FF =  $\sim 0.64$ . High PCEs of  $\sim 4.9\%$  was obtained with the devices using PNDT3NTz-DT ( $p/n = 1:1$ ). Although PNDT3NTz-DT-based devices afford a relatively low FF of  $\sim 0.52$ , they show high  $J_{\text{SC}}$  of  $\sim 11.3$  mA/cm<sup>2</sup> and  $V_{\text{OC}}$  of  $\sim 0.83$  V. Plausible reasons for the higher  $J_{\text{SC}}$  in the devices with PNDT3NTz-DT than with PNDT3BTz-DT may be the wider absorption range and the more intensified absorption (Figure 1). The difference of  $V_{\text{OC}}$  between these two polymers is in good agreement with the difference of IP.

Two-dimensional grazing incidence X-ray diffraction (2D-GIXD) images of pristine polymer films and polymer/PC<sub>61</sub>BM blend films are displayed in Figure 4. In the pristine film deposited on the FDTs-treated Si/SiO<sub>2</sub> substrate, PNDT3BTz-HD gives diffractions corresponding to the lamellar structure along the  $q_z$  axis, with up to the third order, and the  $\pi$ - $\pi$  stacking structure along the  $q_{xy}$  axis at about  $q = 1.8$  Å<sup>-1</sup>,

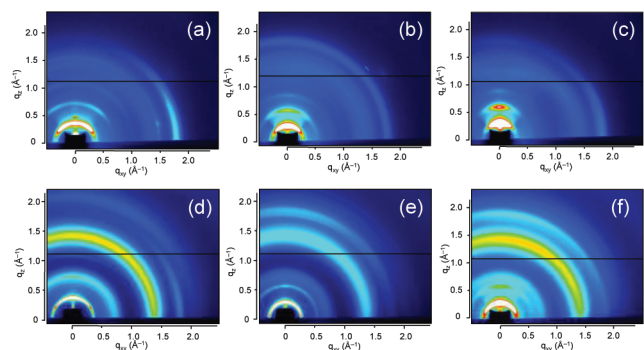


Figure 4. 2D-GIXD images of polymer-only films (a-c) and polymer/PC<sub>61</sub>BM blend films (d-f): (a,d) PNDT3BTz-HD, (b,e) PNDT3BTz-DT, (c,f) PNDT3NTz-DT, where the polymer to PC<sub>61</sub>BM ( $p/n$ ) weight ratios of the blend films are 1:2, 1:1, and 1:1, respectively.

respectively, both as arc, indicative of preferential edge-on orientation (Figure 4a). However, the arcing of diffraction suggests the misorientation of the polymer lamellae, likely owing to the introduction of branched alkyl side chains.<sup>11</sup> PNDT3BTz-DT, with the longer branched side chain, provides  $\pi$ - $\pi$  stacking diffraction as ring, indicating that there is no preferential orientation throughout the film (Figure 4b). It is interesting that, despite the lower orientational order, PNDT3BTz-DT affords higher field-effect mobility than PNDT3BTz-HD. We speculate that this result might be rationalized by the higher solubility and higher molecular weight of PNDT3BTz-DT, which renders better film uniformity and better domain-to-domain connectivity, in turn, facilitating bulk charge transport. In PNDT3NTz-DT, both lamellar and  $\pi$ - $\pi$  stacking diffractions relatively converge to the  $q_z$  and  $q_{xy}$  axes, respectively (Figure 4c), in sharp contrast to PNDT3BTz-DT with the same side chains, indicating a higher tendency of edge-on orientation (though it still forms misoriented regions), which is in good agreement with the higher mobility in PNDT3NTz-DT. This might originate in the symmetry difference between the BTz and NTz core. Having centrosymmetry (NTz), PNDT3NTz-DT provides more straight-shaped backbone than PNDT3BTzs with axisymmetrical BTz core, perhaps leading to the better molecular orientation.<sup>9c</sup> It is noteworthy that the  $\pi$ - $\pi$  stacking distance of all the polymers is estimated to be 3.5 Å, from the in-plane XRD scans (see SI), which is even narrower than that of PNDT3BTs, 3.6 Å,<sup>8</sup> most likely due to the donor-acceptor nature, which enhances intermolecular  $\pi$ - $\pi$  interactions. This narrow  $\pi$ - $\pi$  stacking distance would be one of the reasons for high mobilities in this system.

In the blend films deposited on the ITO/PEDOT/PSS substrate, interestingly, PNDT3BTz-HD preserves the preferential edge-on orientation as the  $\pi$ - $\pi$  stacking diffraction appears on the  $q_{xy}$  axis (Figure 4d), as seen in the polymer-only film. Meanwhile, PNDT3BTz-DT, with longer-branched alkyl side chains, forms an enhanced face-on structure as the  $\pi$ - $\pi$  stacking diffraction appears preferentially on the  $q_z$  axis, though arcing of the diffraction is relatively large (Figure 4e). The face-on rich orientation of PNDT3BTz-DT, which can enhance the out-of-plane charge transport and light absorption, explains the high photovoltaic properties of its cells.<sup>10b,12</sup> PNDT3NTz-DT has almost no preferential orientation, implying the relatively low out-of-plane charge transport, which agrees with low FF of the corresponding cell. Nevertheless, the wider and more intensified absorption would lead to high  $J_{\text{SC}}$  and the larger IP would lead to higher  $V_{\text{OC}}$  in the PNDT3NTz-DT-based cell, respectively, resulting in high PCE of  $\sim 5\%$ .

In summary, we have synthesized a series of novel NDT3-based D-A semiconducting polymers. A striking feature of the present polymers is the very close  $\pi$ - $\pi$  stacking of 3.5 Å, most likely as a result of the large  $\pi$  system and the D-A system in the polymer backbone. PNDT3NTz-DT, in particular, is found to be one of the few examples of versatile polymers that exhibit

both the field-effect mobility of  $\sim 0.5 \text{ cm}^2/(\text{V s})$  and the PCE of  $\sim 5\%$ .<sup>2f,9c</sup> These results indicate that NDT3 is a promising versatile core unit for semiconducting polymers and that the use of highly  $\pi$ -extended heteroarenes both as the donor and the acceptor unit is a promising design strategy to develop high performance polymers.

## ■ ASSOCIATED CONTENT

### ■ Supporting Information

Experimental details and additional supporting figures. This material is available free of charge via the Internet at <http://pubs.acs.org>.

## ■ AUTHOR INFORMATION

### ■ Corresponding Author

\*E-mail: [iosaka@hiroshima-u.ac.jp](mailto:iosaka@hiroshima-u.ac.jp); [ktakimi@hiroshima-u.ac.jp](mailto:ktakimi@hiroshima-u.ac.jp).

### ■ Notes

The authors declare no competing financial interest.

## ■ ACKNOWLEDGMENTS

This work is supported by the Strategic Promotion of Innovative Research and Development from the Japan Science and Technology Agency (JST), the New Energy and Industrial Technology Development Organization (NEDO), and Grants-in-Aid for Young Scientist B (No. 22750172) and Grants-in-Aid for Scientific Research A (No. 23245041) from Japan Society for the Promotion of Science (JSPS). I.O. is also grateful to the JGC-S Scholarship Foundation for financial support. GIXD experiments were performed at the BL19B2 of SPring-8 with the approval of the Japan Synchrotron Radiation Research Institute (JASRI) (Proposal No. 2011B1860).

## ■ REFERENCES

- (1) (a) Skotheim, T. A.; Reynolds, J. R. *Handbook of Conducting Polymers*, 3rd ed.; CRC Press: Boca Raton, FL, 2007. (b) Leclerc, M.; Morin, J.-F. *Design and Synthesis of Conjugated Polymers*; Wiley-VCH Verlag GmbH & Co. KGaA: Weinheim, Germany, 2010.
- (2) (a) Hamadani, B. H.; Gundlach, D. J.; McCulloch, I.; Heeney, M. *Appl. Phys. Lett.* **2007**, *91*, 243512. (b) Umeda, T.; Kumaki, D.; Tokito, S. *J. Appl. Phys.* **2009**, *105*, 024516. (c) Tsao, H. N.; Cho, D.; Andreasen, J. W.; Rouhanipour, A.; Breiby, D. W.; Pisula, W.; Müllen, K. *Adv. Mater.* **2009**, *21*, 209–212. (d) Zhang, W.; Smith, J.; Watkins, S. E.; Gysel, R.; McGehee, M.; Salleo, A.; Kirkpatrick, J.; Ashraf, S.; Anthopoulos, T.; Heeney, M. *J. Am. Chem. Soc.* **2010**, *132*, 11437–11439. (e) Li, Y.; Singh, S. P.; Sonar, P. *Adv. Mater.* **2010**, *22*, 4862–4866. (f) Bronstein, H.; et al. *J. Am. Chem. Soc.* **2011**, *133*, 3272–3275. (g) Tsao, H. N.; Cho, D. M.; Park, I.; Hansen, M. R.; Mavrinskiy, A.; Yoon, D. Y.; Graf, R.; Pisula, W.; Spiess, H. W.; Müllen, K. *J. Am. Chem. Soc.* **2011**, *133*, 2605–2612.
- (3) (a) Liang, Y.; Xu, Z.; Xia, J.; Tsai, S.; Wu, Y.; Li, G.; Ray, C.; Yu, L. *Adv. Mater.* **2010**, *22*, E135–E138. (b) Chen, H. Y.; Hou, J.; Zhang, S.; Liang, Y.; Yang, G.; Yang, Y.; Yu, L.; Wu, Y.; Li, G. *Nat. Photon.* **2009**, *3*, 649–653. (c) Chu, T. Y.; Lu, J.; Beaupré, S.; Zhang, Y.; Pouliot, J. R.; Wakim, S.; Zhou, J.; Leclerc, M.; Li, Z.; Ding, J.; Tao, Y. *J. Am. Chem. Soc.* **2011**, *133*, 4250–4253. (d) Price, S. C.; Stuart, A. C.; Yang, L.; Zhou, H.; You, W. *J. Am. Chem. Soc.* **2011**, *133*, 4625–4631.
- (4) (a) Osaka, I.; Sauv e, G.; Zhang, R.; Kowalewski, T.; McCullough, R. D. *Adv. Mater.* **2007**, *19*, 4160–4165. (b) Zhang, M.; Tsao, H. N.; Pisula, W.; Yang, C.; Mishra, A. K.; Müllen, K. *J. Am. Chem. Soc.* **2007**, *129*, 3472–3473.
- (5) (a) Mhlbacher, D.; Scharber, M.; Morana, M.; Zhu, Z.; Waller, D.; Gaudiana, R.; Brabec, C. *Adv. Mater.* **2006**, *18*, 2884–2889. (b) Blouin, N.; Michaud, A.; Gendron, D.; Wakim, S.; Blair, E.; Neagu-Plesu, R.; Bellet e, M.; Durocher, G.; Tao, Y.; Leclerc, M. *J. Am. Chem. Soc.* **2008**, *130*, 732–742.

- (6) (a) Pan, H.; Li, Y.; Wu, Y.; Liu, P.; Ong, B. S.; Zhu, S.; Xu, G. *J. Am. Chem. Soc.* **2007**, *129*, 4112–4113. (b) Li, J.; Qin, F.; Li, C. M.; Bao, Q.; Chan-Park, M. B.; Zhang, W.; Qin, J.; Ong, B. S. *Chem. Mater.* **2008**, *20*, 2057–2059. (c) Fong, H. H.; Pozdin, V. A.; Amassian, A.; Malliaras, G. G.; Smilgies, D.-M.; He, M.; Gasper, S.; Zhang, F.; Sorensen, M. *J. Am. Chem. Soc.* **2008**, *130*, 13202–13203.
- (7) (a) Shinamura, S.; Miyazaki, E.; Takimiya, K. *J. Org. Chem.* **2010**, *75*, 1228–1234. (b) Shinamura, S.; Osaka, I.; Miyazaki, E.; Nakao, A.; Yamagishi, M.; Takeya, J.; Takimiya, K. *J. Am. Chem. Soc.* **2011**, *133*, 5024–5035. (c) Loser, S.; Bruns, C. J.; Miyauchi, H.; Ortiz, R. P.; Facchetti, A.; Stupp, S. I.; Marks, T. J. *J. Am. Chem. Soc.* **2011**, *133*, 8142–8145. (d) Dutta, P.; Yang, W.; Eom, S. H.; Lee, W. -H.; Kang, I. -N.; Lee, S. -H. *Chem. Commun.* **2012**, *48*, 573–575.
- (8) (a) Osaka, I.; Abe, T.; Shinamura, S.; Miyazaki, E.; Takimiya, K. *J. Am. Chem. Soc.* **2010**, *132*, 5000–5001. (b) Osaka, I.; Abe, T.; Shinamura, S.; Takimiya, K. *J. Am. Chem. Soc.* **2011**, *133*, 6852–6860.
- (9) (a) Mataka, S.; Takahashi, K.; Ikezaki, Y.; Hatta, T.; Tori-i, A.; Tashiro, M. *Bull. Chem. Soc. Jpn.* **1991**, *64*, 68–73. (b) M Wang, M.; Hu, X.; Liu, P.; Li, W.; Gong, X.; Huang, F.; Cao, Y. *J. Am. Chem. Soc.* **2011**, *133*, 9638–9641. (c) Osaka, I.; Shimawaki, M.; Mori, H.; Doi, I.; Miyazaki, E.; Koganezawa, T.; Takimiya, K. *J. Am. Chem. Soc.* **2012**, *134*, 3498–3507.
- (10) (a) Bijleveld, J. C.; Gevaerts, V. S.; Di Nuzzo, D.; Turbiez, M.; Mathijssen, S. G. J.; de Leeuw, D. M.; Wienk, M. M.; Janssen, R. A. J. *Adv. Mater.* **2010**, *22*, E242–E246. (b) Osaka, I.; Saito, M.; Mori, H.; Takimiya, K. *Adv. Mater.* **2012**, *24*, 425–430.
- (11) Osaka, I.; Zhang, R.; Liu, J.; Smilgies, D.-M.; Kowalewski, T.; McCullough, R. D. *Chem. Mater.* **2010**, *22*, 4191–4196.
- (12) (a) Piliago, C.; Holcombe, T. W.; Douglas, J. D.; Woo, C. H.; Beaujuge, P. M.; Fr chet, J. M. J. *J. Am. Chem. Soc.* **2010**, *132*, 7595–7597. (b) He, F.; Wang, W.; Chen, W.; Xu, T.; Darling, S. B.; Strzalka, J.; Liu, Y.; Yu, L. *J. Am. Chem. Soc.* **2011**, *133*, 3284–3287.